



# Effect of Ru on interdiffusion dynamics of $\beta$ -NiAl/DD6 system: A combined experimental and first-principles studies

Zhao Zhang<sup>a</sup>, Bo Bai<sup>a</sup>, Hui Peng<sup>a,b</sup>, Shengkai Gong<sup>a,b</sup>, Hongbo Guo<sup>a,b,\*</sup>

<sup>a</sup> School of Materials Science and Engineering, Beihang University (BUAA), No. 37 Xueyuan Road, Beijing 100191, China

<sup>b</sup> Beijing Key Laboratory for Advanced Functional Material and Thin Film Technology, Beihang University (BUAA), No. 37 Xueyuan Road, Beijing 100191, China

## ARTICLE INFO

### Article history:

Received 30 June 2015

Received in revised form 8 September 2015

Accepted 9 September 2015

Available online 11 September 2015

### Keywords:

Interdiffusion

Ru

NiAl

RuAl

First-principles calculation

## ABSTRACT

As a diffusion barrier between thermal barrier coating (TBC) and advanced single crystal (SC) superalloy DD6, RuNiAl coating has attracted increasing attention recently. In this work, different diffusion couples including NiAl/DD6, RuNiAl/DD6 and RuAl/DD6, were prepared and their interdiffusion behavior was investigated at 1100 °C, to understand the diffusion barrier mechanism of the RuNiAl coating. The addition of Ru to NiAl effectively reduced the interdiffusion coefficient of Al, thereby delaying the phase transformation from  $\beta$  to  $\gamma'$  and suppressing the formation of topologically closed-packed (TCP) phases and primary interdiffusion zone (IDZ). It is verified by first-principles calculations that Ru restrained the formation of Ni and Al vacancies and Ni and Al antisite atoms. According to the calculations, the addition of Ru increases the defect formation energies, thus inhibiting the diffusion of Al in  $\beta$ -NiAl. The calculation results are consistent with the experimental data.

© 2015 Elsevier Ltd. All rights reserved.

## 1. Introduction

The intermetallic compound  $\beta$ -NiAl [1–5] shows promising high temperature applications due to high melting point, low density and good isothermal oxidation resistance, especially as metallic coatings for superalloys or as bond coat in thermal barrier coatings (TBCs) [6–9]. However, owing to the inward diffusion of Al and the outward diffusion of Ni and refractory elements, topologically close-packed (TCP) phases and secondary reaction zone (SRZ) are formed, which significantly accelerates the failure of superalloys and coatings [10–15].

It is reported that the addition of Ru greatly weakens the formation of TCP phases and improved the microstructural stability of the superalloy at high temperature [16–18]. In addition, it is demonstrated that appropriate Ru doping in NiAl was beneficial to its high-temperature oxidation resistance due to the formation of a dense alumina scale [19,20]. Moreover, Ru is also a typical element that can improve the mechanical properties of Ni-base single crystal superalloys [21–23], especially creep strength [24,25]. It is claimed that the high-temperature creep strength of NiAl could be improved by increasing Ru/Ni ratio [26]. The improvement in the creep strength of NiAl can eliminate plastic deformation and suppress crack initiation which is driven by thermal expansion mismatch and results in rumpling and spallation of the alumina scale [27,28].

However, the effect mechanism of Ru in the RuNiAl coating is still unclear, especially as a diffusion barrier. In order to clarify relevant mechanism, some hypotheses have been proposed, including that Ru diffuses very slowly in Ni lattice due to its relatively higher solute-vacancy exchange energy [29]. Besides, Ru has relatively larger atomic radius (~0.134 nm), which leads to the occupation of lattice positions as well as vacancies when it is doped into alloys. Therefore, the vacancy concentration is reduced, and then the vacancy diffusion is restrained in the lattice. Tryon et al. have constructed a Ru-Ni-Al ternary phase diagram to reflect a continuous B2 phase zone between RuAl and NiAl phases at temperatures of 1000 and 1100 °C [30]. The interdiffusion flux of Ni increased the Ru concentration gradient but lowered the Al concentration gradient [31].

Extensive efforts have also been made to investigate Al self-diffusion in NiAl by first-principles calculations. It has suggested that triple defect (TD) mechanism is predominant in Al self-diffusion in stoichiometric and Ni-rich NiAl based on Kirkendall effect at high temperatures [32], while Minamino et al. have pointed out that next nearest neighbor jump (NNN) or Ni-anti-structural bridge (ASB) is the possible mechanism of Al self-diffusion in Ni-rich NiAl [33,34]. Recently, Marino et al. have predicted that the ASB mechanism only contributes to short range Al diffusion and the TD mechanism dominates long range Al diffusion in both Ni-rich and stoichiometric NiAl [35,36].

In our previous work, a (Ru, Ni)Al layer significantly inhibited the inward diffusion of Al from the NiAl coating and the outward diffusion of alloying elements such as W and Mo, thus suppressing the formation of TCP phases and SRZ [37–39]. In order to clarify the influence of Ru on the interdiffusion behavior between the NiAl coating and the underlying

\* Corresponding author at: Beijing Key Laboratory for Advanced Functional Material and Thin Film Technology, Beihang University (BUAA), No. 37 Xueyuan Road, Beijing 100191, China.

E-mail address: [Guo.hongbo@buaa.edu.cn](mailto:Guo.hongbo@buaa.edu.cn) (H. Guo).

**Table 1**  
Nominal composition of single crystal Ni-based superalloy DD6 (in wt.%).

Cr	Ta	Co	W	Mo	Re	Al	Ni
5.18	2.14	9.93	2.82	1.25	1.13	12.00	Bal.

superalloy, interdiffusion coefficients are the most persuasive and necessary.

In this work, the interdiffusion behavior of NiAl/DD6, RuNiAl/DD6 and RuAl/DD6 diffusion couples prepared in vacuum at 1100 °C was investigated. Graphical method according to Boltzmann–Matano theory and defect formation energies calculated by first-principles theory were performed to elucidate the diffusion barrier effect of Ru in  $\beta$ -NiAl.

## 2. Experimental and calculational procedures

### 2.1. Experimental methods

In the present work, Ni-based single crystal superalloy DD6 was used as substrate material. The nominal composition of DD6 is listed in Table 1. The alloy samples were fabricated into dimensions of 4 mm  $\times$  4 mm  $\times$  3 mm, and the sample surfaces were reduced by SiC paper to 2000 grits and polished with 3.5  $\mu$ m alumina powders.

NiAl, RuAl and RuNiAl alloy were prepared by arc-melting Ni (99.99 wt.%), Al (99.99 wt.%) and Ru (99.99 wt.%) rods in a vacuum arc furnace. Heat-treatment of the RuAl and RuNiAl specimens was conducted in vacuum at 1500 °C for 12 h, while NiAl was annealed at 1300 °C for 24 h.

Diffusion couple samples (4 mm  $\times$  4 mm  $\times$  3 mm) were fabricated from the rods by wire-electrode cutting and their surfaces were reduced by SiC paper to 2000 grits and polished with 3.5  $\mu$ m alumina powders. NiAl/DD6, RuAl/DD6 and RuNiAl/DD6 diffusion couples were bound together in a vacuum furnace at 1100 °C and annealed at this temperature for 100 h, with a chamber pressure of about 5 MPa. The microstructures of diffusion couples were characterized by scanning electron microscopy (SEM, Quanta 600) with energy-dispersive X-ray (EDX), and element concentration profiles of diffusion couples were determined by electron probe microanalysis (EPMA, JXA-8100, JEOL).

### 2.2. First-principles calculations

First-principles calculations [40,41] were performed using the Vienna ab initio simulation package (VASP) code with the Perdew–Burke–Ernzerhof (PBE) [42] version of Generalized Gradient Approximation (GGA) proposed by Perdew and Wang for exchange–correlation functional. The kinetic energy cutoff for the plane-wave basis was set as 350 eV which was sufficient to keep total energy convergence at 1 meV/atom or less. First-order Methfessel–Paxton smearing was used to handle partial occupancies, required for metallic systems and a Fermi surface smearing width of 0.2 eV resulted in an entropy term of less than 1 meV atom<sup>−1</sup>. Nuclear positions were relaxed using a

conjugate gradient algorithm until the forces on all the atoms were converged to less than 10<sup>−2</sup> eV/Å.

Defect formation energies of isolated defects and defect clusters were ensured by testing the size of the supercell. Until the defect formation energy was converged to within a 0.1 eV tolerance, the supercell size was deemed suit to avoid interactions between periodic images of the defects model [43]. A 128-atom 4  $\times$  4  $\times$  4 supercell was used for calculating the Ni triple defect mechanism clusters. A 54-atom 3  $\times$  3  $\times$  3 supercell was required for point defects and the Al Next Nearest Neighbor and the Al six-jump cycle mechanisms. For the *k*-point sampling [44] of the Brillouin zone, the Monkhorst–Pack scheme was used. A 6  $\times$  6  $\times$  6 *k*-point mesh was sufficient to give fully converged results for triple defect mechanism, was different from others, a 8  $\times$  8  $\times$  8 *k*-points mesh was used.

First, we confirmed that the optimized lattice parameter for  $\beta$ -NiAl primitive cell was 2.896 Å which was identical to Marino et al.'s calculation results [43] and within 5% of experimental value of 2.887 Å [44]. The volume change of NiAl associated with the addition of Ru was neglected due to the low concentration of Ru, which was not larger than 0.1 at.%.

In a Ru–NiAl alloy, we can reasonably assume that the defect contents are sufficiently dilute to allow use of the Wagner–Schottky model [45] for researching the point defect concentrations as a function of alloy composition and temperature. It is convenient to use the atomic concentration to define the defect concentration, it can be obtained by Eq. (1),

$$x_{i_a} = \frac{n_{i_a}}{N_{atom}} \quad (1)$$

Here,  $N_{atom}$  is the total number of atoms and  $n_{i_a}$  is the number of species *i* on the  $\alpha$  sublattice with  $i = \{Al, Ni, Ru, Va\}$  and  $\alpha = \{Al, Ni\}$ .

In the Wagner–Schottky model, the formation enthalpy of B2 Ru–NiAl alloy is a linear function of the defect concentration, like in Eq. (2):

$$\Delta H_d^f = \Delta H_{NiAl}^f + \sum_d H_d x_d, \quad (2)$$

where  $\Delta H_{NiAl}^f$  is the formation enthalpy of stoichiometric NiAl,  $H_d$  is the formation enthalpy of defects with  $d = \{Va_{Ni}, Va_{Al}, Al_{Ni} \text{ and } Ni_{Al}\}$ , and  $x_d$  is the defect concentration. At zero pressure, enthalpy and energy are equivalent, so Eq. (2) can be replaced as Eq. (3):

$$E_d = \frac{(\Delta E_d^f - \Delta E_{NiAl}^f)}{x_d} \quad (3)$$

Here,  $\Delta E_d^f$  is the formation energy of an alloy, which is calculated by Eq. (4) for NiAl, and by Eq. (5) for Ru–NiAl alloy, as follows.  $\Delta E_{NiAl}^f$  is the formation energy of a pure NiAl with no defect, which is calculated by Eq. (4), where  $x = 0.5$ . According to Eq. (1), for only one type of defect,  $x_d$  is one divided by the total number of atoms in the supercell.

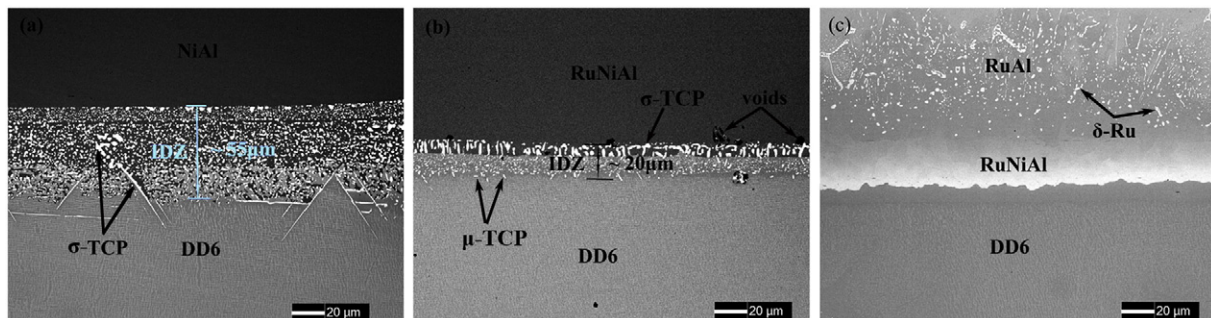


**Fig. 1.** SEM micrographs of cross-sections of NiAl/DD6 (a), RuNiAl/DD6 (b), and RuAl/DD6 (c) diffusion couples after 100 h heat-treatment in vacuum at 1100 °C.

Download English Version:

<https://daneshyari.com/en/article/7220216>

Download Persian Version:

<https://daneshyari.com/article/7220216>

[Daneshyari.com](https://daneshyari.com)